
In-Context Learning of Large Language Models Explained as Kernel Regression

Chi Han, Ziqi Wang, Han Zhao, Heng Ji
University of Illinois Urbana-Champaign
{chihan3, ziqiw9, hanzhao, hengji}@illinois.edu

Abstract

Large language models (LLMs) have initiated a paradigm shift in transfer learning. In contrast to the classic pretraining-then-finetuning procedure, in order to use LLMs for downstream prediction tasks, one only needs to provide a few demonstrations, known as in-context examples, without adding more or updating existing model parameters. This in-context learning (ICL) capabilities of LLMs is intriguing, and it is not yet fully understood how pretrained LLMs acquire such capabilities. In this paper, we investigate the reason why a transformer-based language model can accomplish in-context learning after pre-training on a general language corpus by proposing one hypothesis that LLMs can simulate kernel regression algorithms when faced with in-context examples. More concretely, we first prove that Bayesian inference on in-context prompts can be asymptotically understood as kernel regression $\hat{y} = \frac{\sum_i y_i K(x, x_i)}{\sum_i K(x, x_i)}$ as the number of in-context demonstrations grows. Then, we empirically investigate the in-context behaviors of language models. We find that during ICL, the attentions and hidden features in LLMs match the behaviors of a kernel regression. Finally, our theory provides insights on multiple phenomena observed in ICL field: why retrieving demonstrative samples similar to test sample can help, why ICL performance is sensitive to the output formats, and why ICL accuracy benefits from selecting in-distribution and representative samples. We will make our code available to the research community following publication.

1 Introduction

Pre-trained large language models (LLMs) have emerged as powerful tools in the field of natural language processing, demonstrating remarkable performance across a broad range of applications [21, 8, 22, 2, 9]. They have been used to tackle diverse tasks such as text summarization, sentiment analysis, schema induction and translation, among others [2, 15, 9]. One of the most fascinating capabilities of LLMs is their ability to perform in-context learning (ICL), a process in which a language model can make predictions on a test sample based on a few demonstrative examples provided in the input context [11]. This feature makes LLMs particularly versatile and adaptive to different tasks. Studies have found ICL to emerge especially when the size of LLM is large enough, and pre-trained over a massive corpus [23].

Although intuitive for human learners, ICL poses a mystery for optimization theories because of the significant format shift between ICL prompts and pre-training corpus. There have been lots of efforts in providing a theoretical understanding of how LLMs implement ICL. Some work [25, 19] approaches this problem from a data perspective: they claim that ICL is possible if a model masters Bayesian inference on pre-training distribution. However, they fail to explain how such inference is feasibly implemented in practical language models, nor did their theory provide insights into ICL behaviors. Another stream of work conjectures that under a simple linear setting: $[x, y]$ where $y = w^\top x$ and the input sequence x only has length 1, they can construct a Transformer [17] to

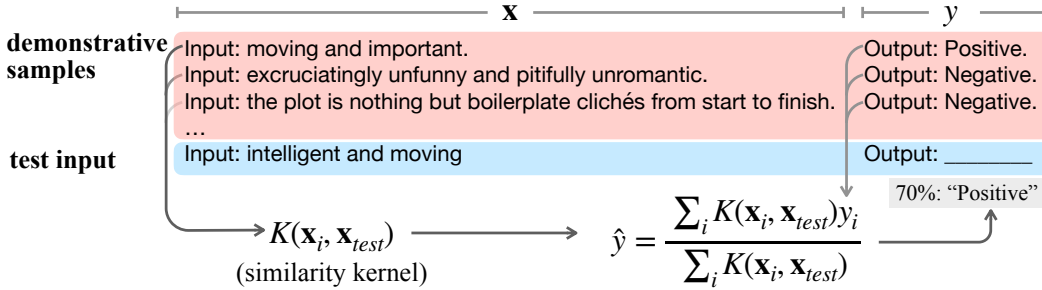


Figure 1: Our results suggests that LLMs might be conducting kernel regression on ICL prompts.

implement gradient descent (GD) algorithm over ICL prompt [1, 18, 5]. However, this constrained setting diverges from the most interesting part of ICL, as state-of-the-art LLMs work with linguistic tasks where the sequential textual inputs has complex semantic structures, and ICL emerges from pre-training on general-purpose corpus instead of explicit ICL training.

In this work, we delve deeper into the question of *what mechanism enables Transformer-based LLMs to, after pre-training on a general language corpus, accomplish in-context learning on sequential data*. We specifically explore the hypothesis that LLMs employ a kernel regression algorithm when confronted with in-context prompts. Kernel regression adopts a non-parametric form

$$\hat{y} = \frac{\sum_i y_i K(x, x_i)}{\sum_i K(x, x_i)} \quad (1)$$

when making predictions, where $K(x, x_i)$ is a kernel that measures the similarity between inputs x and x_i . In plain words, it estimates the output \hat{y} on x by drawing information from similar other data points x_i and take a weighted sum on their y_i .

We first provide a theoretical analysis demonstrating that Bayesian inference predictions on in-context prompts converge to a kernel regression in Section 4. Our results also shed light on various phenomena observed in previous empirical studies, such as the advantage of retrieving in-context examples that are similar to the test sample, the sensitivity of ICL performance to the output formats, and why using a group of in-distribution and representative samples improves ICL accuracy.

Following our theoretical investigation, in Section 5 we conduct empirical studies to verify our explanation of in-context learning of LLMs in more details. Our results reveal that during LLM ICL, the attention map used by the last token to predict the next token is allocated in accordance with our explanation. By plugging attention values into our equation, we are also able to reconstruct the model’s output by over 80% accuracy. Moreover, we are able to reveal how information necessary to kernel regression is computed in intermediate LLM layers. In conclusion, we make the following contributions in this work:

- We provide a theoretical explanation of how practical LLMs can be capable of ICL using the concept of kernel regression.
- We conduct empirical analysis to verify that the LLM’s attention maps and hidden features matches our explanation.
- Our theoretical explanation provides insights and heuristics to multiple phenomena observed in ICL practice by previous studies.

2 Related Work

2.1 In-Context Learning

As an intriguing property of large language models, in-context learning has attracted high attention in research community. There have been numerous studies on empirical analysis of in-context learning, including format and effects of in-context samples [14, 13, 27], selection of in-context

samples [10, 12], characteristics of in-context learning behaviors [27, 12, 7, 23], and relation between ICL and pre-training dataset [24, 3].

Going deeper, researchers have also been interested in building a theoretical understanding of why ICL works. One branch of studies investigates ICL from a data perspective: [26, 19] demonstrate that a good enough Bayesian inference on pre-training data might cause emergence of ICL ability. However they fail to explain if such Bayesian inference is computationally feasible in practical language models, as such Bayesian inference involves unbounded depth computational graphs as the number of samples increases. Our study builds on top of some similar assumptions, but goes further to explain how ICL can be accomplished with attention-mechanism in Transformers [17].

Another angle of explanation is analyzing what algorithms might be implemented in LLMs for ICL, which is closely related to our study. Representative studies include [1, 5, 18, 4], with the majority of them proposing gradient descent (GD) algorithm as a promising candidate answer. However, attempts in explicit construction of GD algorithm in Transformers [1, 18] mostly assume an oversimplified setting of linear tasks with input length equal to 1, and evaluate Transformers after training on a synthetic dataset (including [1, 5]). This is different from ICL’s main advantage as an emergent ability on language pre-training, and that LLMs are able to work on textual data which involves more complex syntactic and semantic structures.

2.2 Emergent Ability of LLMs

This is a larger topic that in-context learning is also highly related to. [21, 2, 8, 22] showed that abilities including reasoning, in-context learning, few-shot learning, instruction understanding and multilingualism emerge in large language models after pre-training on massive language data. These impressive and mysterious capacities have boosted significant progress in natural language processing as well as artificial intelligence, but still baffle theoretical analysis. In this work, we make a preliminary step towards understanding ICL as a special case of LM capacity emergence.

3 Formulation

3.1 Preliminaries: Hidden Markov Models

Following the setting of [25], we assume that the pre-training corpus can be modelled by a mixture of HMMs. Each HMM corresponds to a certain task $\theta \in \Theta$. Assuming a large finite number of tasks, one can include all task-specific HMMs into one single HMM. In this unified HMM, let \mathcal{S} be the set of states, and \mathcal{O} be the set of observations where $|\mathcal{O}| = m$. At each time step, state s_t randomly emits one observation o_t and then transits to the next state s_{t+1} . $p_{\text{pre-train}}, P(s_{t+1} = s' | s_t = s)$ and $P(o_t = o | s_t = s)$ denote the pre-training initial distribution, transition distribution and emission distribution respectively. Under an arbitrary ordering of \mathcal{S} and \mathcal{O} , we can define the transition matrix $T : T(s, s') = P(s' | s)$, and emission matrix $B : B(s, o) = P(o | s)$, respectively. We also let $\mathbf{o} = (o_0, \dots)$ be the full observation sequence, and $\mathbf{o}_{[0:l]}$ denote its first l tokens.

3.2 In-Context Learning

In this work we consider the following formulation of in-context learning (ICL). Let Θ be the set of tasks. The distribution of sequences generated by each individual task in the HMM together composes the pre-training distribution. Specifically, each task $\theta \in \Theta$ is associated with a distinct initial state $s_\theta \in \mathcal{S}$, and the set of all such initial states $\mathcal{S}_{\text{start}} = \{s_\theta | \theta \in \Theta\}$ forms the support of $p_{\text{pre-train}}$.

Following the ICL prompt formulation in [25], for a test task θ^* , the in-context learning prompt follows the format:

$$[S_n, \mathbf{x}_{\text{test}}] = [\mathbf{x}_1, y_1, o^{\text{delim}}, \mathbf{x}_2, y_2, o^{\text{delim}}, \dots, \mathbf{x}_n, y_n, o^{\text{delim}}, \mathbf{x}_{\text{test}}], \quad (2)$$

where the input-output pairs $[\mathbf{x}_i, y_i]$ are i.i.d. demonstrate samples sampled from θ^* , and o^{delim} is delimiter token used to separate adjacent samples.

We further make some connections between in-context learning and the HMM model. Note that the probability of generating a sequence from the initial distribution p_0 can be expressed as follows[6]:

$$P(\mathbf{o}_{[0:l]}|p_0) = \mathbf{v}_{p_0}^\top \left(\prod_{i=0}^{l-1} \text{diag}(\mathbf{p}_{o_i})T \right) \text{diag}(\mathbf{p}_{o_l})\mathbf{1}, \quad (3)$$

where $\mathbf{p}_{(o)}$ is vector of emission probabilities $P(o|s \in \mathcal{S})$. We denote the intermediate matrices as one operator $T_{\mathbf{o}_{[0:l-1]}} = \prod_{i=0}^{l-1} \text{diag}(\mathbf{p}_{o_i})T$. We can use a matrix $\Sigma_{p,l}$ to denote the covariance between all of its d^2 elements of $\text{vec}(T_{\mathbf{o}_{[0:l-1]}})$ when $\mathbf{o}_{[0:l-1]}$ is generated from initial distribution p . For each individual task, we also have $\epsilon_\theta = \inf_l \rho(\Sigma_{p_{\text{pre-train}}}^{-1} - \Sigma_{s_\theta,l}^{-1})$ to quantify the difference between sequences generated by s_θ and those from pre-training distribution, where ρ denotes the spectral radius of a matrix. Let $\eta = \sup_{\mathbf{o}_{[0:l-1]}} \|T_{\mathbf{o}_{[0:l]}}\|_F$ be the upper bound of $T_{\mathbf{o}_{[0:l]}}$'s Frobenius-norm.

3.3 Assumptions

We go on and present the assumptions we make on the formulation:

Assumption 1. (Recurrence) *If a sequence \mathbf{o} is generated by task θ , then s_θ can be revisited in future steps with non-zero probability:*

$$\forall \mathbf{o}_{[0:l-1]}, P(s_t = s_\theta | \mathbf{o}_{[0:l-1]}, \theta) \geq \epsilon_r,$$

Remark: this means that the pre-training corpus is of a repetitive nature, and the task θ 's "theme" is repeatedly mentioned or discussed throughout a text sequence.

Assumption 2. (Beginning Anchor Words) *The beginning token of any sequence has non-zero emission probability only on starting states:*

$$\forall \mathbf{o} \sim p_{\text{pre-train}}, s \notin \mathcal{S}_{\text{start}}, P_O(o_0|s) = 0$$

Remark: this means that the start of a sentence is usually indicative enough, such as the start of a new line combined with capital letters at the beginning of a paragraph.

Assumption 3. (Delimiter Emission Probability) *Each state $s \in \mathcal{S}$ has bounded probability of generating o^{delim} :*

$$P_O(o^{\text{delim}}|s) \geq \epsilon_d.$$

Remark: this means that the delimiter token has probability to be generated unexpectedly, and reflects the common linguistic phenomenon of "elliptical construction", where people stop at a partially completed sentence as long as the omitted part can be inferred from the context.

Assumption 4. (Distinguishability) *The Kullback–Leibler divergence (KL divergence) between the first l tokens between two distinct tasks $\theta \neq \theta'$ is lower-bounded by:*

$$\inf_{\theta, \theta'} D_{KL}(P(\mathbf{o}_{[0:l]}|\theta') || P(\mathbf{o}_{[0:l]}|\theta)) = \epsilon_{KL} > \ln \frac{1}{\epsilon_r \epsilon_d}.$$

Remark: this requires that tasks are distinguishable enough from each other. As KL-divergence is non-decreasing with length l , this assumption also encourages the length l to be large enough to provide sufficient task-specific information.

Assumption 5. (Bounded Task Deviation) *The in-context learning tasks should not deviate too much from the pre-training corpus:*

$$\epsilon_\theta < \frac{\Delta}{2\eta^2}$$

where $\Delta = \inf_{y' \neq y_{\max}} |P(y_{\max} | \mathbf{x}_{\text{test}}) - P(y' | \mathbf{x}_{\text{test}})|$ is the minimum margin in test sample prediction.

Remark: this assumption requires that the sentences in each task should not significantly deviate from general pre-training distribution, a phenomenon also known as linguistic regularity.

4 Theoretical Analysis

4.1 Explaining ICL as Kernel Regression

Within the framework presented in Section 3, we pose the following result. The basic idea is that, as the number of samples n increases, inference on the in-context learning prompt converges to a kernel-regression form.

Theorem 1. *With any probability $1 - \delta$, if the in-context prompt is larger than a threshold*

$$n > n_\delta = O(\text{poly}(\ln m, \ln \frac{1}{\delta}, \ln \frac{1}{\epsilon_d}, \ln \frac{1}{\epsilon_r}, (\epsilon_{KL} - \ln \frac{1}{\epsilon_r \epsilon_d})^{-1}, (\frac{\Delta}{2} - \epsilon_\theta \eta^2)^{-1})),$$

then the most probable prediction by posterior inference

$$\arg \max_y P(y | S_n, \mathbf{x}_{test})$$

equals to the one with maximal value in the following kernel regression form

$$\arg \max \frac{\sum_{i=1}^n \mathbf{e}(y_i) \langle \text{vec}(T_{\mathbf{x}_{test}}), \Sigma_{p_{pre-train}}^{-1} \text{vec}(T_{\mathbf{x}_i}) \rangle}{\sum_{i=1}^n \langle \text{vec}(T_{\mathbf{x}_{test}}), \Sigma_{p_{pre-train}}^{-1} \text{vec}(T_{\mathbf{x}_i}) \rangle} \quad (4)$$

where $\langle \cdot, \cdot \rangle$ indicates the inner product, and $\mathbf{e}(y)$ is the one-hot vector corresponding to index y .

Equation 4 can be interpreted as follows: it calculates the semantic similarity between the test input \mathbf{x}_{test} and each sample \mathbf{x}_i , and aggregates their outputs to compute a most likely prediction for the test sample. This is natural to the motivation of ICL: we encourage the LLM to leverage the pattern provided in demonstrative samples, and mimic the pattern to predict on the test input. Equation 4 is also similar to the form of attention mechanism used in Transformer decoder models:

$$h = \text{softmax}(q^\top K) V^\top = \frac{\sum_j v_j e^{\langle q, k_j \rangle}}{\sum_j e^{\langle q, k_j \rangle}} \quad (5)$$

where q is the query vector corresponding to the last token, k, K are the key vectors and matrix, and v, V are the value vectors and matrix used in the Transformer, respectively. The only difference is that $e^{\langle q, k_i \rangle}$ is replaced with a dot product in Equation 4, which can be regarded as a kernel trick. We assume that previous hidden layers are responsible for learning the semantic vectors of samples inputs $\text{vec}(T_{\mathbf{x}})$. We can then make the following loose analogy between our kernel regression explanation (Equation 4) and the attention mechanism (Equation 5):

- Label information $\mathbf{e}(y_i)$ corresponds with the *value* vector v_i
- The similarity kernel $\langle \text{vec}(T_{\mathbf{x}_{test}}), \Sigma_{p_{pre-train}}^{-1} \text{vec}(T_{\mathbf{x}_i}) \rangle$ loosely corresponds to the attention value $e^{\langle q, k_i \rangle}$, where:
- the semantic information $\text{vec}(T_{\mathbf{x}_i})$ corresponds to the *key* vectors k_i and *query* vectors q_i for samples $[\mathbf{x}, y]$.

One might argue that it is also theoretically possible to directly infer the next token in matrix form $p_{pre-train}^\top T_{[S_n, \mathbf{x}_{test}]}$. However, this form involves $2n$ consecutive matrix multiplications. When n increases, this is infeasible for a practical Transformer architecture which is composed of a fixed number of layers. In comparison, Equation 4 only requires semantic information for each sample \mathbf{x} to be provided beforehand, and the applies kernel regression (which can be done by one attention layer) to get the answer. Learning to represent $T_{\mathbf{x}}$ is probable for preceding layers, as it is also used for ordinary inference $P(y|\mathbf{x}) = p_{pre-train}^\top T_{\mathbf{x}}$. In experiments in Section 5 we demonstrate that this analogy can explain the ICL behaviors of LLMs to an extent.

4.2 Insights Provided by the Explanation

Theorem 1 is able to explain multiple phenomena in ICL field that are observed by previous studies. This is helpful for understanding and predicting the behaviors of ICL, and providing heuristics for future development.

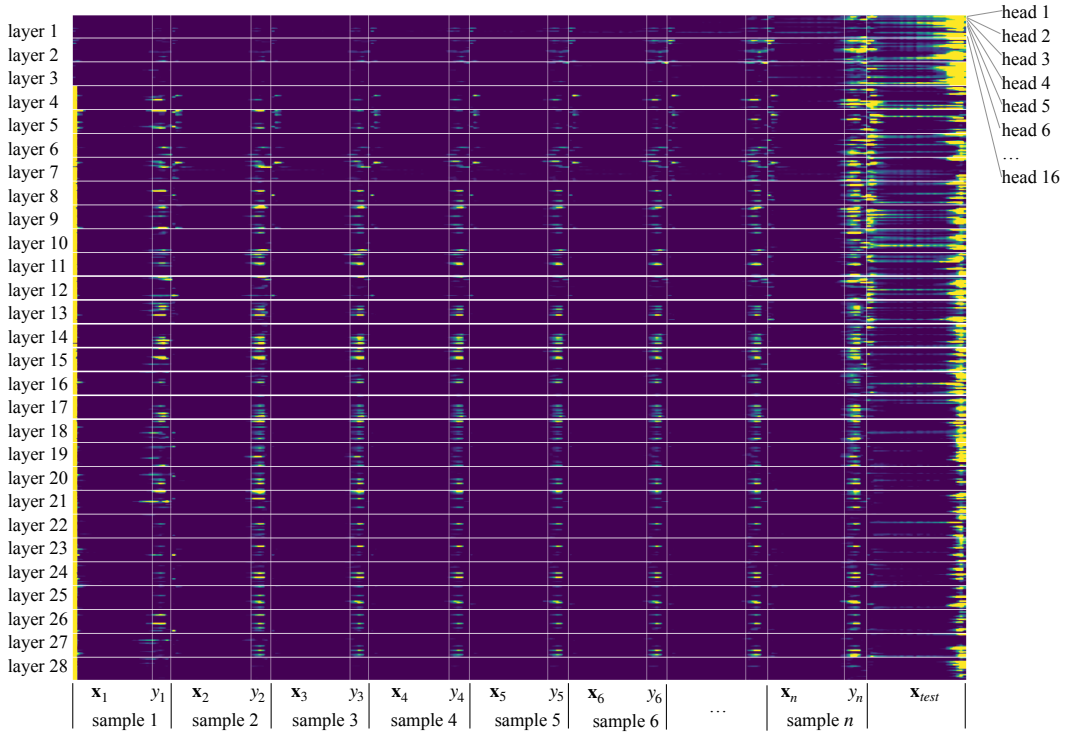


Figure 2: Averaged attention map over GLUE-sst2 test set. A portion of attentions on demonstrative samples are generally focused on label positions y_i . This conforms to the intuition in kernel regression explanation in Theorem 1 that the inference on in-context learning prompts is a weighted average over sample labels.

Retrieving Similar Samples It is empirically observed [16, 10] that retrieving demonstrative samples \mathbf{x}_i that are similar to the test input \mathbf{x}_{test} can benefit ICL performance. This phenomenon is understandable from our explanation. Encouraging selection of similar samples can be understood as limiting the cosine distance between demonstrative samples \mathbf{x}_i and test sample \mathbf{x}_{test} in sentence embedding space. This is similar to selecting a smaller “bandwidth” in kernel regression and sampling only from a local window, which reduces the bias in kernel regression. Therefore, devising better retrieval technique for selecting samples, especially those with similar representations as LLMs, is a promising direction for further boosting ICL scores.

Sensitivity to Label Format [14] also observes that the ICL performance relies on the label format. Replacing the label set with another random set will reduce the performance of ordinary auto-regressive LLMs. This can be explained in our theory that the model’s output comes from a weighted voting of demonstrative sample labels $\{y_i\}$. If the label space is changed the next token will also be misled to a different output space. So it is generally beneficial for ICL to ensure the demonstrative samples and test samples share an aligned label space and output format.

Sample Inputs’ Distribution Another phenomenon discovered by previous studies is the importance of sample inputs’ distribution [14], where out-of-distribution (OOD) demonstrative samples will degrade ICL accuracy. This mirrors our Assumptions 5 that the demonstrations $[\mathbf{x}_i, y_i]$ should be sampled in a way close to $p_{\text{pre-train}}$. Our theory also encourages that the samples should form a representative set in the input space. Otherwise if there are distributional difference from samples \mathbf{x}_i and the task θ^* , a bias or instability in the estimation in Equation 4 will be introduced. In all, this insight supports the importance that high quality and representative demonstrations be sampled.

Remaining Challenges However, we need to point out that there are still phenomena not explainable by our framework, as well as most previous explanations. One most mysterious one is the

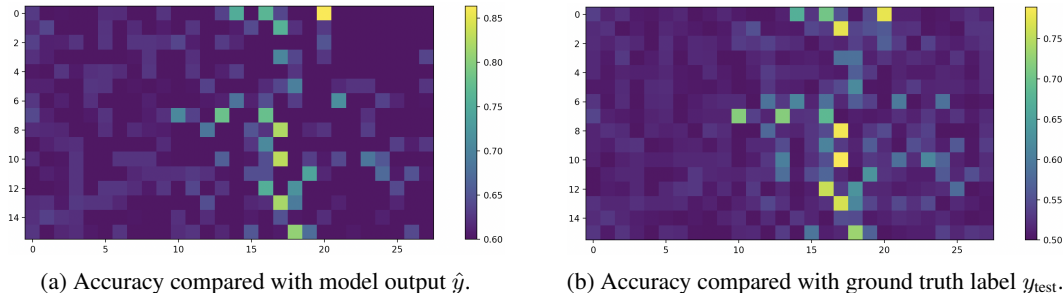


Figure 3: We use each head’s attention weights on demonstrative samples to manually average sample labels y_i . x -axis are layers and y -axis are heads in each layer. These figures show that this “reconstructed” output in some heads from layers 16~21 matches LLM prediction with as high as 89.2% accuracy, and matches ground truth with 86.4% accuracy.

sensitivity to sample ordering [12] as a kernel regression should be order-ignorant, which no existing explanations (including [25, 1]) take into account. Another unexplained phenomenon is LLM’s robustness to perturbed or random labels [14]. We attribute such phenomena to the fact that LLMs also rely on a large portion of implicit reasoning in text generation, and might benefit from linguistic cues in text prompt. Our theory provides partial explanation, which needs to be combined with this implicit ability of LLMs to form a more comprehensive understanding of ICL.

5 Empirical Analysis

In this section we conduct empirical analysis on LLMs in order to verify our hypothesis. Because Equation 4 is only one special solution among infinite many of its equivalent forms, and it also relies on the unknown HMM structure, it is infeasible to directly evaluate it on data. However, we can verify if it can predict observable behaviors on LLMs in experiments. In this section, unless otherwise stated, we run GPT-J 6B model¹ on one Tesla V100. It employs a decoder-only Transformer architecture. In this section, we use the validation set of sst2 dataset as a case study, while results on more tasks can be found at Appendix B. GPT-J-6B ICL achieves 89.6% accuracy on the test set. We investigate the ICL behavior of LLMs from shallow to deep levels, and sequentially ask the following 4 questions: does the attention heads collect label information $e(y_i)$ as predicted? Does the attention-kernel analogy explain LLM’s prediction? Can we actually explain the attention values as a kind of similarity? Can we find where algorithmic features $e(y_i), T_{x_i}$ are stored? The following sections answer these questions one by one.

5.1 Where Are Attentions Distributed During ICL?

First, we notice that Equation 2 implies that the LLM takes a weighted average over sample labels y_i in ICL. Figure 2 shows how attention weights are distributed on in-context learning inputs $[S_n, \mathbf{x}_{\text{test}}]$. On each test point, we sample one ICL prompt, and collect the attention map over previous tokens for predicting the next token. After getting the attention maps, as ICL samples \mathbf{x}_i may have varied lengths, we re-scale the attentions on each \mathbf{x} from $|\mathbf{x}|$ to a fixed 30-token length with linear interpolation. After aligning the attention lengths, we average all attention maps. The horizontal axis is the aligned positions on prompt $[S_n, \mathbf{x}_{\text{test}}]$. Each bar corresponds to one of 28 Transformer layers. Within each bar, each thin line is 1 out of 16 attention heads. Darker (blue) areas mean smaller averaged attention, while brighter areas indicate high attention.

In Figure 2, there are three major locations of attention masses. First, a majority of attentions are focused on the final few tokens in \mathbf{x}_{test} , especially in the first 3 layers. This accords with previous observations that Transformer attentions tend to locate in a local window to construct local semantic feature for \mathbf{x}_{test} . Secondly, as also observed in previous studies, LLMs tend to allocate much attention on the first few tokens in a sequence to collect starter information. Finally and most intriguingly, we observe concentrated attention on each sample label tokens $\{y_i\}$. This phenomenon confirms an aggregation of label information in LLM ICL, in line with the prediction by Equation 4.

¹https://huggingface.co/docs/transformers/model_doc/gptj

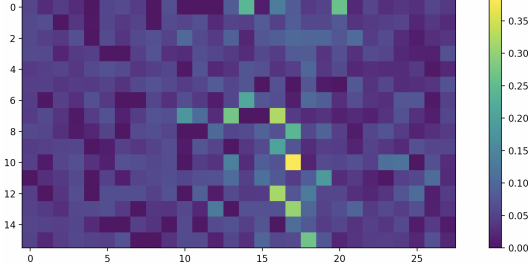


Figure 4: Pearson correlation between sample’s attentions and *prediction similarity* $\text{sim}_{\text{pred}}(\mathbf{x}_{\text{test}}, \mathbf{x}_i)$ (Equation 6). Note the resemblance between this heatmap and Figure 3.

5.2 Can Attentions Be Interpreted as Kernel Functions?

Now that we observe expected locations of attention weights on labels, we go on to verify if the LLM really predicts by averaging on labels as suggested by Theorem 1. We iterate over 16 heads and 28 layers, and insert their attention weights into Equation 4 to manually average the label distribution. This is similar in concept to a mind reading experiment to predict one’s next word using brain waves only [20]. Specifically, for each attention head, we use the maximal attention value a_i within the range of $[\mathbf{x}_i, y_i]$ as the kernel weight. Then on the ICL samples, we reconstruct the a prediction as follows:

$$\tilde{y} = \arg \max \frac{\sum_{i=1}^n \mathbf{e}(y_i) a_i}{\sum_{i=1}^n a_i}$$

The resulting “reconstructed output” \tilde{y} is compared for both LLM’s actual prediction \hat{y} and ground truth label y_{test} to calculate its accuracy. Figure 3a and 3b plot the accuracy between \tilde{y} and \hat{y} and between \tilde{y} and y_{test} respectively. Interestingly, we spot the existence of several heads in layers 18~21 which demonstrate high accuracy in reconstruction. The highest of them (layer 17, head 10) achieves 89.2% accuracy on \hat{y} and 86.4% accuracy on y_{test} . This result validates our hypothesis that some components in Transformer-based LLMs implement kernel regression. Note that this phenomenon happens within a few adjacent layers in the middle of the model. This is similar to our prediction in Section 4.1: not many attention layers are needed for kernel regression, as long as the required features have been computed by preceding layers. It is enough for the higher layers to only pass on the computed results.

5.3 Which Samples Receive High Attention?

We go on and ask the question: if the LLMs use attention to implement kernel regression, *what kind of similarity does this kernel function evaluate?* From Equation 4, we see that the dot product is measuring similarity between $T_{\mathbf{x}}$, which encodes information necessary for HMM inference: $p(o|\mathbf{x}) = p_{\text{pre-train}}^{\top} T_{\mathbf{x}} B$. Therefore, we conjecture that the attention value a_i between \mathbf{x}_{test} and \mathbf{x}_i correlates with their prediction similarity. Specifically, we define the *prediction similarity* as follows:

$$\text{sim}(\mathbf{x}_1, \mathbf{x}_2) = P(o|\mathbf{x}_1)^{\top} P(o|\mathbf{x}_2), \quad (6)$$

which is measured by applying LLMs on these texts *alone*, rather than in ICL prompt. Finally, we compute the Pearson correlation coefficient between $\text{sim}(\mathbf{x}_{\text{test}}, \mathbf{x}_i)$ and each attention values on samples for each attention head. The results are shown in Figure 4. The absolute value of correlation is not high, as $P(o|\mathbf{x})$ is a dimension reduction to $T_{\mathbf{x}}$ and can lose and mix information. However, we can still note a striking similarity between it and Figure 3. This means that the heads responsible for ICL mostly attend to *prediction-similar* samples.

5.4 Do Intermediate Features Store Information Useful for Kernel Regression?

Finally, we go into a more detailed level, and investigate the question: *where do Transformer-based LMs store the algorithmic information needed by kernel regression?* To this end, we take out the intermediate *key* and *value* features in all layer heads, and see if the correct information is stored in correct locations. Note in Section 5.1, we observe that a major part of attention weights are located at the label position, so we focus on positions within $[-1, 3]$ relative to this position. Noticing

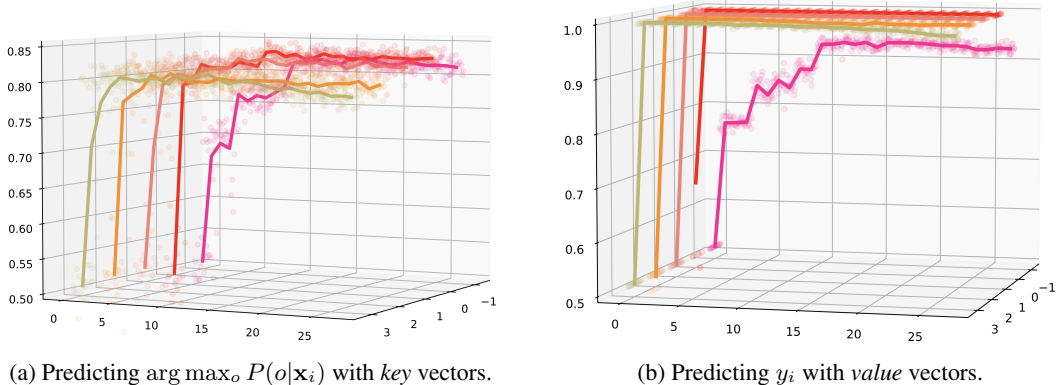


Figure 5: Key and value vectors encode label and LLM prediction information at high-attention position. Here x-axis (0~27) is layer number, y-axis denotes relative position to the high-attention position within each demonstration, and z-axis is accuracy. Each sphere is an attention head. The curve shows average accuracy within each layer.

the analogy we made at Section 4.1 that $k_i \sim \text{vec}(T_{x_j})$ and $v_j \sim y_j$, we study two sub-questions: (1) whether *value* vectors encode label information y_i ; and (2) whether *key* vectors encode LLM prediction information $P(o|x_i)$. For each head, we conduct Ridge regression with $\lambda = 0.01$ to fit the task in these 2 questions. Results are presented in Figure 5. We can observe that, generally the high-attention position (y-axis = 0) indeed achieves best accuracy. Figure 5b is intuitive, as tokens at a position later than the label token y_i can easily access the information of y_i by self attention. The slight drop at position +3 means that a longer distance introduces more noise to this information flow. Results in Figure 5a tells us that, although sentence x_i 's starting position in ICL prompt is shifted and different from 0, k_i is still strongly correlated with $P(o|x_i)$, which indicates a sense of translation invariance. Overall, the results mean that, with the attention map distributed in Figure 2, LLM is able to use attention mechanism to extract information regarding T_{x_i} and y_i from *key* and *value* vectors effectively just as we described.

6 Conclusions and Future Work

In conclusion, our work provides a novel theoretical view to understand the intriguing in-context learning (ICL) capabilities of Transformer-based large language models (LLMs). We propose that LLMs can simulate kernel regression algorithms when dealing with in-context examples. Our empirical investigations into the in-context behaviors of LLMs reveal that the model's attentions and hidden features during ICL are congruent with the behaviors of kernel regression. Furthermore, our theory also explains several observable phenomena in the field of ICL: why the retrieval of demonstrations similar to the test sample can enhance performance, the sensitivity of ICL to output formats, and the improvements in ICL accuracy when selecting in-distribution and representative samples. There are still remaining challenges in this topic, such as understanding the effect of sample orderings and the robustness to perturbed labels. These questions, along with understanding other perspectives of LLMs, are exciting questions for future research.

7 Limitations

There are still spaces for improvement in the quest for understanding the emergent ICL capacity of LLMs. As described in Section 4.2, several phenomena still baffles theoretical characterization, such as the sensitivity to sample orders and robustness to input-label mismatch. We conjecture that answering this question requires deeper understanding of LLMs' ability in representation and implicit reasoning. Moreover, in this study we focus on the category of classification tasks where the output involves only one token. Although more complex tasks such as generation, translation and question answering can be viewed as a sequence of classification tasks, a more direct way to analyze text output is much desired. Finally, this study utilizes a well-established but also simple framework of HMM, which is inconvenient for modelling the complicated nature of natural language and we call for better theoretical frameworks for linguistic analysis.

Acknowledgements

This work was supported in part by US DARPA KAIROS Program No. FA8750-19-2-1004 and AIDA Program No. FA8750-18-2-0014. The views and conclusions contained in this document are those of the authors and should not be interpreted as representing the official policies, either expressed or implied, of the U.S. Government. The U.S. Government is authorized to reproduce and distribute reprints for Government purposes notwithstanding any copyright notation here on.

References

- [1] Ekin Akyürek, Dale Schuurmans, Jacob Andreas, Tengyu Ma, and Denny Zhou. What learning algorithm is in-context learning? investigations with linear models. In *The Eleventh International Conference on Learning Representations*, 2023.
- [2] Tom Brown, Benjamin Mann, Nick Ryder, Melanie Subbiah, Jared D Kaplan, Prafulla Dhariwal, Arvind Neelakantan, Pranav Shyam, Girish Sastry, Amanda Askell, et al. Language models are few-shot learners. *Advances in neural information processing systems*, 33:1877–1901, 2020.
- [3] Stephanie Chan, Adam Santoro, Andrew Lampinen, Jane Wang, Aaditya Singh, Pierre Richemond, James McClelland, and Felix Hill. Data distributional properties drive emergent in-context learning in transformers. *Advances in Neural Information Processing Systems*, 35:18878–18891, 2022.
- [4] Damai Dai, Yutao Sun, Li Dong, Yaru Hao, Shuming Ma, Zhifang Sui, and Furu Wei. Why can gpt learn in-context? language models implicitly perform gradient descent as meta-optimizers. In *ICLR 2023 Workshop on Mathematical and Empirical Understanding of Foundation Models*, 2022.
- [5] Shivam Garg, Dimitris Tsipras, Percy Liang, and Gregory Valiant. What can transformers learn in-context? a case study of simple function classes. In *Advances in Neural Information Processing Systems*, 2023.
- [6] Herbert Jaeger. Observable operator models for discrete stochastic time series. *Neural computation*, 12(6):1371–1398, 2000.
- [7] Daniel Khashabi, Chitta Baral, Yejin Choi, and Hannaneh Hajishirzi. Reframing instructional prompts to gptk’s language. In *Findings of the Association for Computational Linguistics: ACL 2022*, pages 589–612, 2022.
- [8] Takeshi Kojima, Shixiang Shane Gu, Machel Reid, Yutaka Matsuo, and Yusuke Iwasawa. Large language models are zero-shot reasoners. In *Advances in Neural Information Processing Systems*, 2023.
- [9] Sha Li, Ruining Zhao, Manling Li, Heng Ji, Chris Callison-Burch, and Jiawei Han. Open-domain hierarchical event schema induction by incremental prompting and verification. In *Proc. The 61st Annual Meeting of the Association for Computational Linguistics (ACL2023)*, 2023.
- [10] Jiachang Liu, Dinghan Shen, Yizhe Zhang, William B Dolan, Lawrence Carin, and Weizhu Chen. What makes good in-context examples for gpt-3? In *Proceedings of Deep Learning Inside Out (DeeLIO 2022): The 3rd Workshop on Knowledge Extraction and Integration for Deep Learning Architectures*, pages 100–114, 2022.
- [11] Robert Logan IV, Ivana Balažević, Eric Wallace, Fabio Petroni, Sameer Singh, and Sebastian Riedel. Cutting down on prompts and parameters: Simple few-shot learning with language models. In *Findings of the Association for Computational Linguistics: ACL 2022*, pages 2824–2835, 2022.
- [12] Yao Lu, Max Bartolo, Alastair Moore, Sebastian Riedel, and Pontus Stenetorp. Fantastically ordered prompts and where to find them: Overcoming few-shot prompt order sensitivity. In *Proceedings of the 60th Annual Meeting of the Association for Computational Linguistics (Volume 1: Long Papers)*, pages 8086–8098, 2022.

- [13] Sewon Min, Mike Lewis, Hannaneh Hajishirzi, and Luke Zettlemoyer. Noisy channel language model prompting for few-shot text classification. In *Proceedings of the 60th Annual Meeting of the Association for Computational Linguistics (Volume 1: Long Papers)*, pages 5316–5330, 2022.
- [14] Sewon Min, Xinxi Lyu, Ari Holtzman, Mikel Artetxe, Mike Lewis, Hannaneh Hajishirzi, and Luke Zettlemoyer. Rethinking the role of demonstrations: What makes in-context learning work? *arXiv preprint arXiv:2202.12837*, 2022.
- [15] Alec Radford, Jeffrey Wu, Rewon Child, David Luan, Dario Amodei, Ilya Sutskever, et al. Language models are unsupervised multitask learners. 2023.
- [16] Ohad Rubin, Jonathan Herzig, and Jonathan Berant. Learning to retrieve prompts for in-context learning. In *Proceedings of the 2022 Conference of the North American Chapter of the Association for Computational Linguistics: Human Language Technologies*, pages 2655–2671, 2022.
- [17] Ashish Vaswani, Noam Shazeer, Niki Parmar, Jakob Uszkoreit, Llion Jones, Aidan N Gomez, Łukasz Kaiser, and Illia Polosukhin. Attention is all you need. *Advances in neural information processing systems*, 30, 2017.
- [18] Johannes von Oswald, Eyvind Niklasson, Ettore Randazzo, João Sacramento, Alexander Mordvintsev, Andrey Zhmoginov, and Max Vladymyrov. Transformers learn in-context by gradient descent. *arXiv preprint arXiv:2212.07677*, 2022.
- [19] Xinyi Wang, Wanrong Zhu, and William Yang Wang. Large language models are implicitly topic models: Explaining and finding good demonstrations for in-context learning. *arXiv preprint arXiv:2301.11916*, 2023.
- [20] Zhenhailong Wang and Heng Ji. Open vocabulary electroencephalography-to-text decoding and zero-shot sentiment classification. In *Proc. Thirty-Sixth AAAI Conference on Artificial Intelligence (AAAI2022)*, 2022.
- [21] Jason Wei, Yi Tay, Rishi Bommasani, Colin Raffel, Barret Zoph, Sebastian Borgeaud, Dani Yogatama, Maarten Bosma, Denny Zhou, Donald Metzler, et al. Emergent abilities of large language models. *Transactions on Machine Learning Research*, 2022.
- [22] Jason Wei, Xuezhi Wang, Dale Schuurmans, Maarten Bosma, Fei Xia, Ed H Chi, Quoc V Le, Denny Zhou, et al. Chain-of-thought prompting elicits reasoning in large language models. In *Advances in Neural Information Processing Systems*, 2022.
- [23] Jerry Wei, Jason Wei, Yi Tay, Dustin Tran, Albert Webson, Yifeng Lu, Xinyun Chen, Hanxiao Liu, Da Huang, Denny Zhou, et al. Larger language models do in-context learning differently. *arXiv preprint arXiv:2303.03846*, 2023.
- [24] Yuhui Wu, Felix Li, and Percy S Liang. Insights into pre-training via simpler synthetic tasks. *Advances in Neural Information Processing Systems*, 35:21844–21857, 2022.
- [25] Sang Michael Xie, Aditi Raghunathan, Percy Liang, and Tengyu Ma. An explanation of in-context learning as implicit bayesian inference. In *International Conference on Learning Representations*, 2022.
- [26] Wanying Xie. Gx at semeval-2021 task 2: Bert with lemma information for mcl-wic task. In *Proceedings of the 15th International Workshop on Semantic Evaluation (SemEval-2021)*, pages 706–712, 2021.
- [27] Zihao Zhao, Eric Wallace, Shi Feng, Dan Klein, and Sameer Singh. Calibrate before use: Improving few-shot performance of language models. In *International Conference on Machine Learning*, pages 12697–12706. PMLR, 2021.

A Proofs

Proof. First, we denote the kernel regression function

$$\hat{\mathbf{y}} = \frac{1}{n} \sum_{i=1}^n \langle \text{flat}(T_{\mathbf{x}_{\text{test}}}), \Sigma_{p_0}^{-1} \text{flat}(T_{\mathbf{x}_i}) \rangle \mathbf{e}(y_i),$$

In expectation,

$$\mathbb{E}_{\mathbf{x}_i} \langle \text{flat}(T_{\mathbf{x}_{\text{test}}}), \Sigma_{p_{\theta^*}}^{-1} \text{flat}(T_{\mathbf{x}_i}) \rangle \text{flat}(T_{\mathbf{x}_i})^\top = \text{flat}(T_{\mathbf{x}_{\text{test}}}) \Sigma_{p_{\theta^*}}^{-1} \mathbb{E}_{\mathbf{x}_i} \text{flat}(T_{\mathbf{x}_i}) \text{flat}(T_{\mathbf{x}_i})^\top = \text{flat}(T_{\mathbf{x}_{\text{test}}})^\top.$$

As flat is a linear function, for the original matrix:

$$\mathbb{E}_{\mathbf{x}_i} \langle \text{flat}(T_{\mathbf{x}_{\text{test}}}), \Sigma_{p_{\theta^*}}^{-1} \text{flat}(T_{\mathbf{x}_i}) \rangle T_{\mathbf{x}_i} = T_{\mathbf{x}_{\text{test}}}^{\mathcal{F}}$$

Han [What is the RHS of the equation above? It has not been properly defined so far.] and then

$$\begin{aligned} & \mathbb{E}_{\mathbf{x}_i} \langle \text{flat}(T_{\mathbf{x}_{\text{test}}}), \Sigma_{p_{\theta^*}}^{-1} \text{flat}(T_{\mathbf{x}_i}) \rangle P(y = Y | \mathbf{x}_i, p_{\theta^*}) \\ &= P(y = Y | \mathcal{S})^\top \mathbb{E}_{\mathbf{x}_i} \langle \text{flat}(T_{\mathbf{x}_{\text{test}}}), \Sigma_{p_{\theta^*}}^{-1} \text{flat}(T_{\mathbf{x}_i}) \rangle T_{\mathbf{x}_i} p_{\theta^*} \\ &= P(y = Y | \mathcal{S})^\top T_{\mathbf{x}_{\text{test}}} p_{\theta^*} \\ &= P(y = Y | \mathbf{x}_{\text{test}}, \theta^*) \end{aligned}$$

As $(\mathbf{x}_i, \mathbf{e}(y_i))$ can be seen as independent samples on $P(y = Y | \mathbf{x}_i, p_{\theta^*})$, we can use Hoeffding's inequality and bound that, with $1 - \frac{\delta}{2}$ probability,

$$\|\hat{\mathbf{y}} - P(y = Y | \mathbf{x}_{\text{test}}, \theta^*)\|_\infty \leq \sqrt{\frac{1}{2n} \ln \frac{4m}{\delta}}$$

To incorporate the effect of difference between $\Sigma_{p_{\theta^*}}$ and Σ_{p_0} we see that for any matrices $T_1^{\mathcal{F}}, T_2^{\mathcal{F}}$,

$$\begin{aligned} & | \langle \text{flat}(T_{\mathbf{x}_{\text{test}}}), \Sigma_{p_{\theta^*}}^{-1} \text{flat}(T_{\mathbf{x}_i}) \rangle - \langle \text{flat}(T_{\mathbf{x}_{\text{test}}}), \Sigma_{p_0}^{-1} \text{flat}(T_{\mathbf{x}_i}) \rangle | \\ &= | \text{flat}(T_{\mathbf{x}_{\text{test}}})^\top (\Sigma_{p_{\theta^*}}^{-1} - \Sigma_{p_0}^{-1}) \text{flat}(T_{\mathbf{x}_i}) | \\ &\leq \eta^2 \epsilon_\theta \end{aligned}$$

Therefore,

$$\|\hat{\mathbf{y}} - P(y = Y | \mathbf{x}_{\text{test}}, \theta^*)\|_\infty \leq \sqrt{\frac{1}{2n} \ln \frac{4m}{\delta}} + \eta^2 \epsilon_\theta$$

Next we bridge $P(y = Y | \mathbf{x}_{\text{test}}, \theta^*)$ with $P(y = Y | [S_n, \mathbf{x}_{\text{test}}], p_{\text{pre-train}})$. Let s_{test} be the hidden state corresponding to first token of \mathbf{x}_{test} , i.e., $\mathbf{x}_{\text{test},0}$. We see that, the likelihood of $s_{\text{test}} = s_{\theta^*}$ is lower bounded by:

$$\begin{aligned} P(s_{\text{test}} = s_{\theta^*}, S_n | p_{\text{pre-train}}) &= \sum_{\theta \in \Theta} P(s_{\text{test}} = s_{\theta^*} | S_n, s_\theta) P(S_n | s_\theta) P(s_\theta | p_{\text{pre-train}}) \\ &\quad (\text{by Assumption 1}) = P(s_{\text{test}} = s_{\theta^*} | S_n, s_{\theta^*}) P(S_n | s_{\theta^*}) P(s_{\theta^*} | p_{\text{pre-train}}) \\ &\quad (\text{also by Assumption 1}) \geq P(S_n | s_{\theta^*}) P(s_{\theta^*} | p_{\text{pre-train}}) \epsilon_r \\ &\quad (\text{Markov property}) \geq \left(\prod_{i=1}^n P([\mathbf{x}_i, y_i, o^{\text{delim}}] | s_{\theta^*}) P(s_{\theta^*} | [\mathbf{x}_i, y_i, o^{\text{delim}}], s_{\theta^*}) \right) P(s_{\theta^*} | p_{\text{pre-train}}) \epsilon_r \\ &\quad (\text{by Assumption 1,3}) \geq \left(\prod_{i=1}^n P([\mathbf{x}_i, y_i] | s_{\theta^*}) \epsilon_d \epsilon_r \right) P(s_{\theta^*} | p_{\text{pre-train}}) \epsilon_r \\ &\geq \left(\prod_{i=1}^n P([\mathbf{x}_i, y_i] | s_{\theta^*}) \right) P(s_{\theta^*} | p_{\text{pre-train}}) \epsilon_r^{n+1} \epsilon_d^n \end{aligned}$$

For another task θ' , s_{test} is unlikely to be $s_{\theta'}$ because:

$$\begin{aligned}
P(s_{\text{test}} = s_{\theta'}, S_n | p_{\text{pre-train}}) &= \sum_{\theta \in \Theta} P(s_{\text{test}} = s_{\theta'} | S_n, s_{\theta}) P(S_n | s_{\theta}) P(s_{\theta} | p_{\text{pre-train}}) \\
&\text{(by Assumption 1)} = P(s_{\text{test}} = s_{\theta'} | S_n, s_{\theta'}) P(S_n | s_{\theta'}) P(s_{\theta'} | p_{\text{pre-train}}) \\
&\text{(by Assumption 2)} \leq \left(\prod_{i=1}^n P([\mathbf{x}_i, y_i, o^{\text{delim}}] | \theta') \right) P(s_{\theta'} | p_{\text{pre-train}}) \\
&\leq \left(\prod_{i=1}^n P([\mathbf{x}_i, y_i] | \theta') \right) P(s_{\theta'} | p_{\text{pre-train}})
\end{aligned}$$

Therefore, the Bayesian inference over s_{test} , is:

$$\begin{aligned}
&P(s_{\text{test}} = s_{\theta^*} | [S_n, \mathbf{x}_{\text{test}}], p_{\text{pre-train}}) \\
&= \frac{P(s_{\text{test}} = s_{\theta^*}, S_n | p_{\text{pre-train}})}{P(S_n | p_{\text{pre-train}})} \\
&= \frac{P(s_{\text{test}} = s_{\theta^*}, S_n | p_{\text{pre-train}})}{\sum_{\theta} P(s_{\text{test}} = s_{\theta}, S_n | p_{\text{pre-train}})} \\
&= \left(\sum_{\theta} \frac{\left(\prod_{i=1}^n P([\mathbf{x}_i, y_i] | \theta') \right) P(s_{\theta'} | p_{\text{pre-train}})}{P(s_{\theta^*}, S_n | p_{\text{pre-train}})} \right)^{-1} \\
&\geq \left(1 + \min_{\theta \neq \theta^*} \exp \left(\sum_{i=1}^n \ln \frac{P([\mathbf{x}_i, y_i] | \theta)}{P([\mathbf{x}_i, y_i] | \theta^*)} + n \ln \frac{1}{\epsilon_d} + (n+1) \ln \frac{1}{\epsilon_r} + \ln \frac{1}{\|p_0\|_{-\infty}} \right) \right)^{-1} \\
\text{(with } 1 - \frac{\delta}{2} \text{ prob.)} &\geq \left(1 + \min_{\theta \neq \theta^*} \exp \left(-n\epsilon_{KL} + \sqrt{\frac{1}{n} \ln \frac{4}{\delta}} + n \ln \frac{1}{\epsilon_d} + (n+1) \ln \frac{1}{\epsilon_r} + \ln \frac{1}{\|p_0\|_{-\infty}} \right) \right)^{-1} \\
&\geq 1 - \exp \left(-n\epsilon_{KL} + \sqrt{\frac{1}{n} \ln \frac{4}{\delta}} + n \ln \frac{1}{\epsilon_d} + (n+1) \ln \frac{1}{\epsilon_r} + \ln \frac{1}{\|p_0\|_{-\infty}} \right)
\end{aligned}$$

When

$$n > \max \left(\frac{\ln \frac{4m}{\delta}}{2(\frac{\Delta}{2} - \epsilon_{\theta} \eta^2)^2}, \frac{\ln \frac{2}{\frac{\Delta}{2} - \epsilon_{\theta} \eta^2} + \ln \frac{1}{\epsilon_d \epsilon_r (\|p_0\|_{-\infty})} + 1}{\epsilon_{KL} - \ln \frac{1}{\epsilon_d \epsilon_r}} \right),$$

we have:

$$\|\hat{\mathbf{y}} - P(Y | [S_n, \mathbf{x}_{\text{test}}], p_{\text{pre-train}})\|_{\infty} < \frac{\Delta}{2}$$

So that $\forall y' \neq y_{\text{max}}$,

$$\hat{\mathbf{y}}(y_{\text{max}}) - \hat{\mathbf{y}}(y') > \Delta - \frac{\Delta}{2} - \frac{\Delta}{2} = 0.$$

Therefore, the most likely prediction is still y_{max} .

□

B Results on more tasks

Besides the case study on SST2 dataset in Section 5, in this section we also provide experiment results on other tasks. In specific, we experiment on Rotten Tomatoes², Tweet Eval³'s (hate, irony and offensive subtasks) and MNLI⁴. The results are as follows.

B.1 Rotten Tomatoes

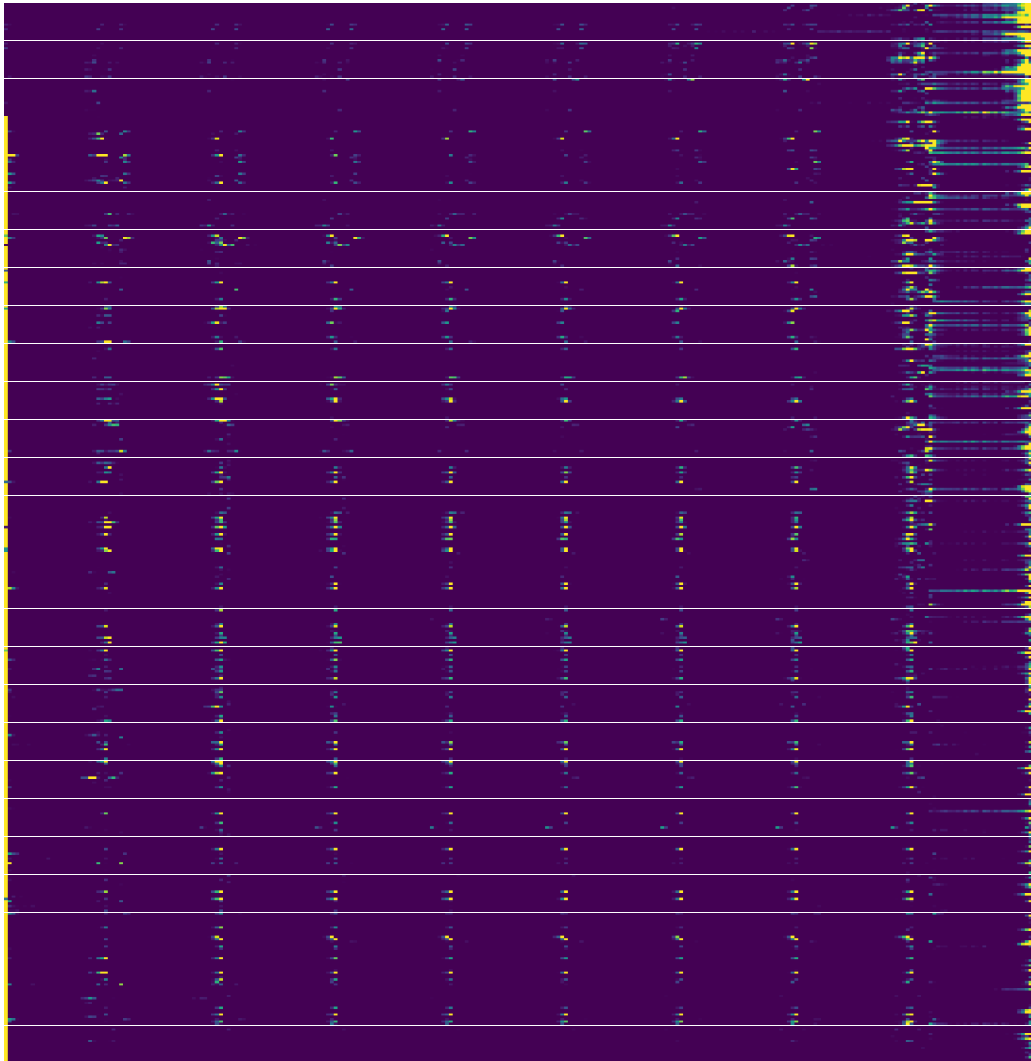
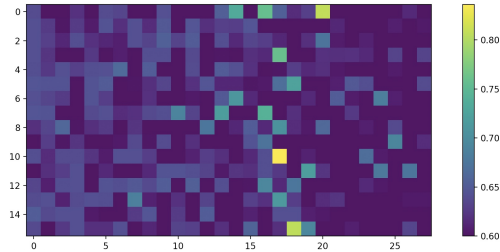


Figure 6: Averaged attention map over Rotten Tomatoes test set.

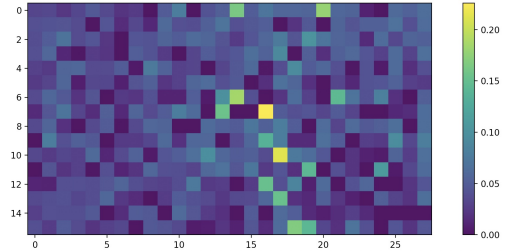
²https://huggingface.co/datasets/rotten_tomatoes/

³https://huggingface.co/datasets/tweet_eval/

⁴https://huggingface.co/datasets/glue/viewer/mnli_matched/test

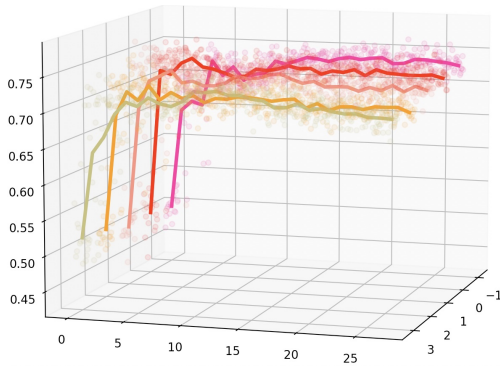


(a) Accuracy on reconstruction of \hat{y} by interpreting attention as kernel weights.

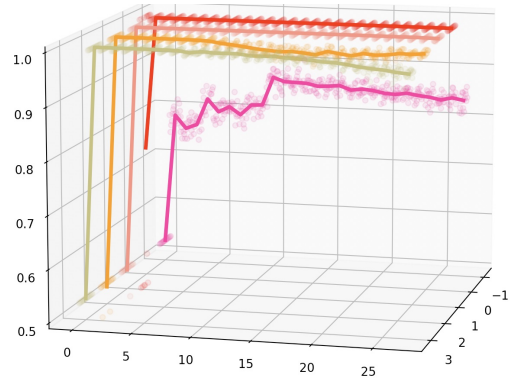


(b) Pearson correlation between attention and logit similarity.

Figure 7: Interpreting attention values from kernel regression perspective on Rotten Tomatoes dataset.



(a) Predicting $\arg \max_o P(o|x_i)$ with *key* vectors.



(b) Predicting y_i with *value* vectors.

Figure 8: Investigating information in key and value vectors on Rotten Tomatoes dataset.

B.2 Tweet Eval (Hate)

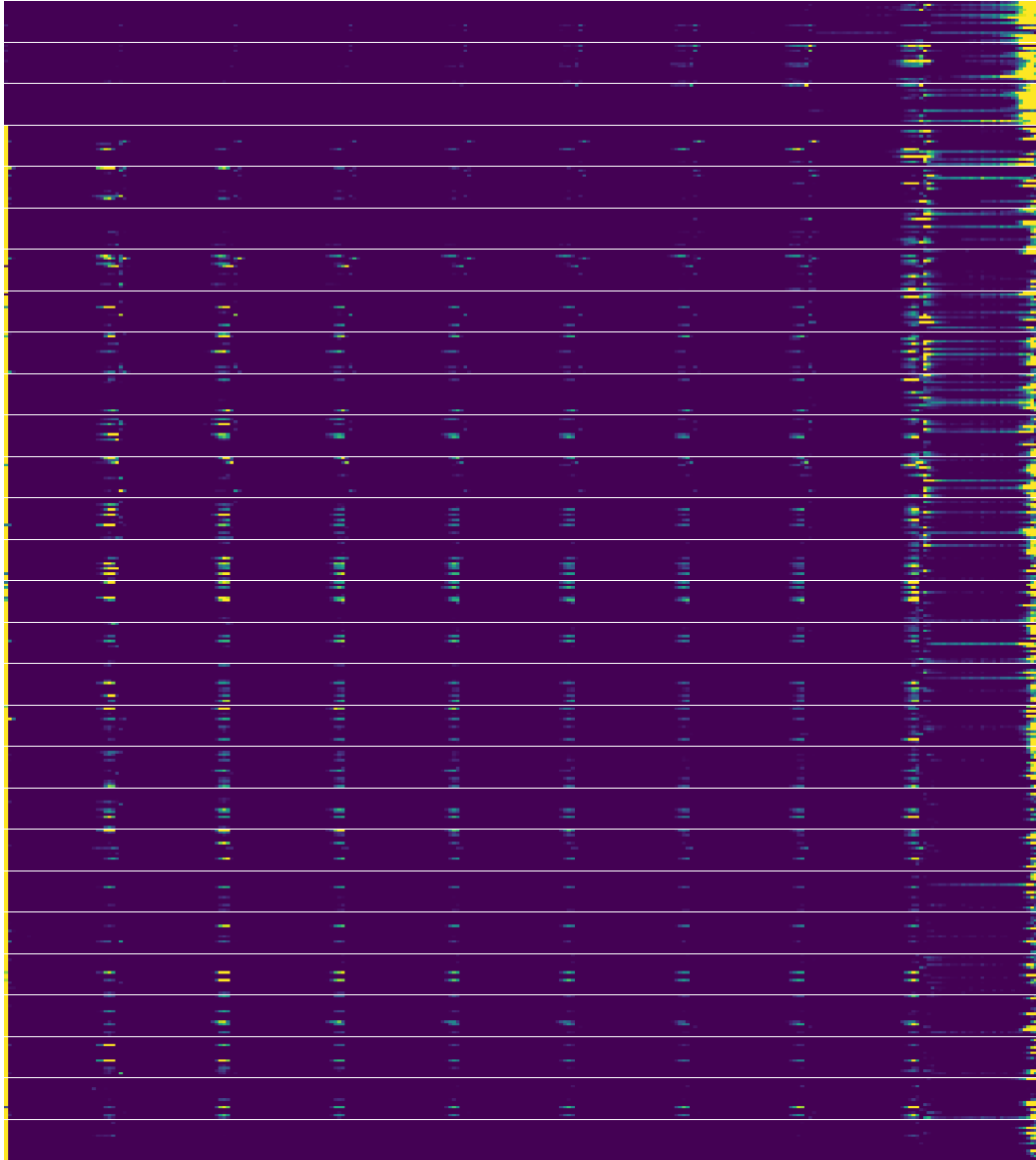
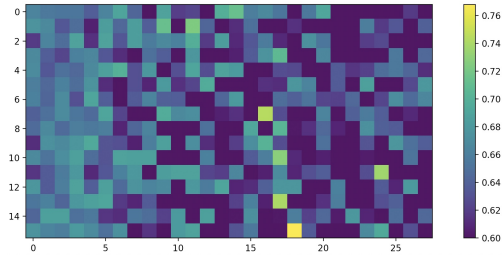
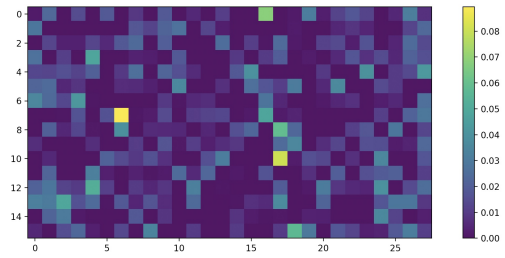


Figure 9: Averaged attention map over Tweet Eval (Hate) test set.

B.3 Tweet Eval (Irony)

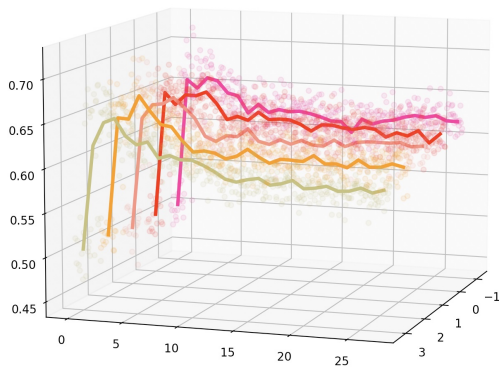


(a) Accuracy on reconstruction of \hat{y} by interpreting attention as kernel weights.

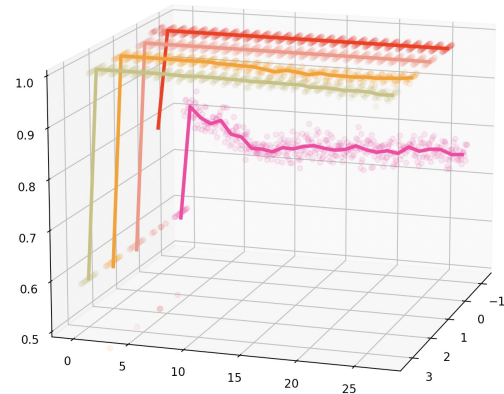


(b) Pearson correlation between attention and logit similarity.

Figure 10: Interpreting attention values from kernel regression perspective on Tweet Eval (Hate) dataset.



(a) Predicting $\arg \max_o P(o|x_i)$ with *key* vectors.



(b) Predicting y_i with *value* vectors.

Figure 11: Investigating information in key and value vectors on Tweet Eval (Hate) dataset.

B.4 Tweet Eval (Offensive)

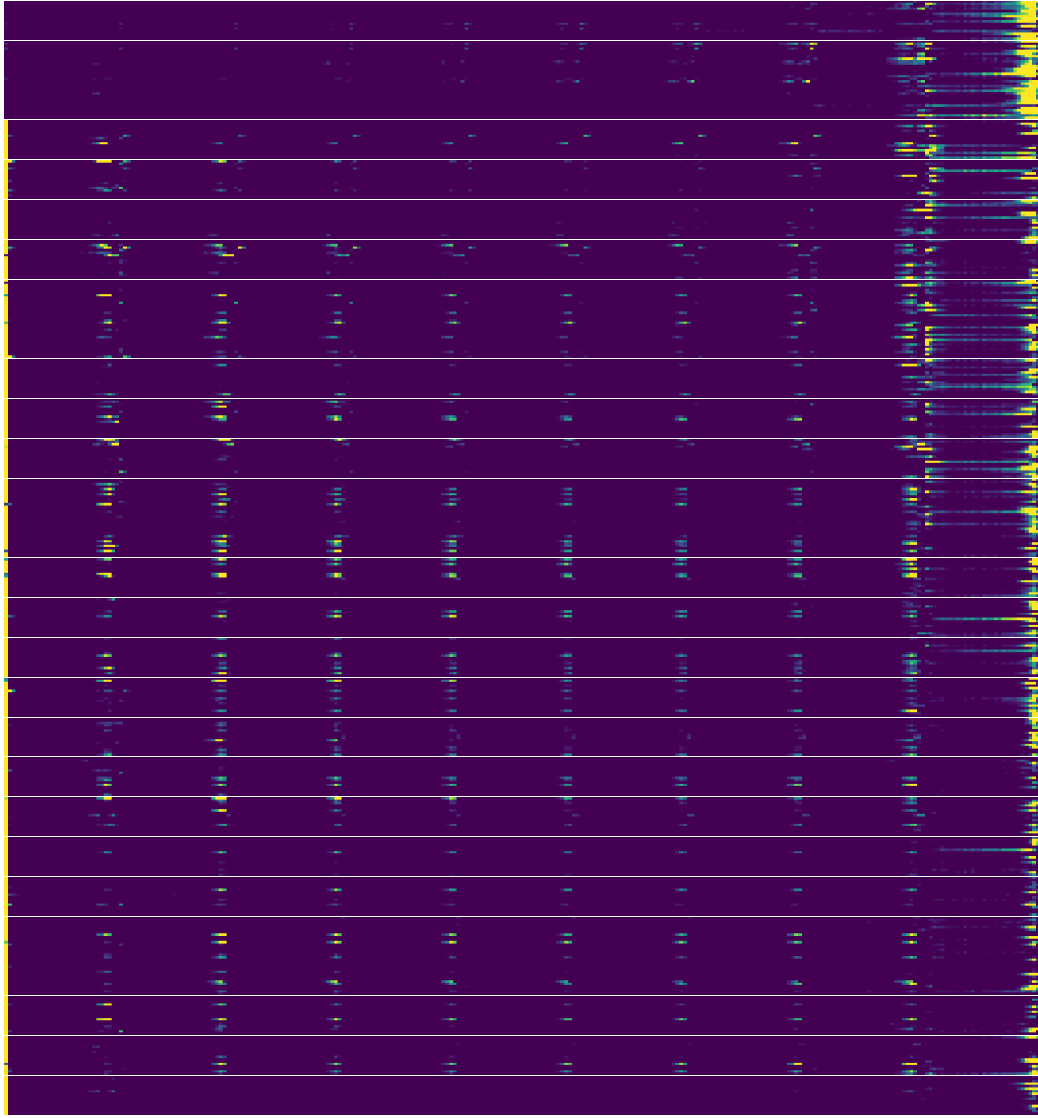
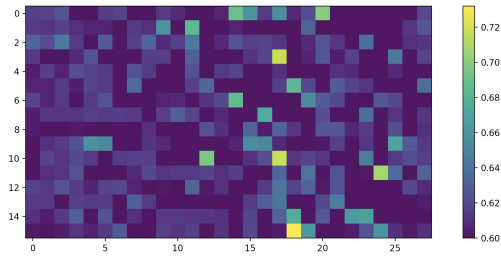
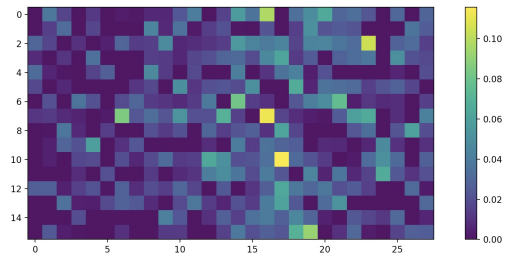


Figure 12: Averaged attention map over Tweet Eval (Irony) test set.

B.5 MNLI

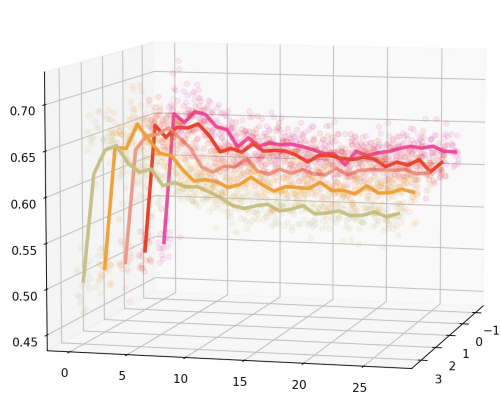


(a) Accuracy on reconstruction of \hat{y} by interpreting attention as kernel weights.

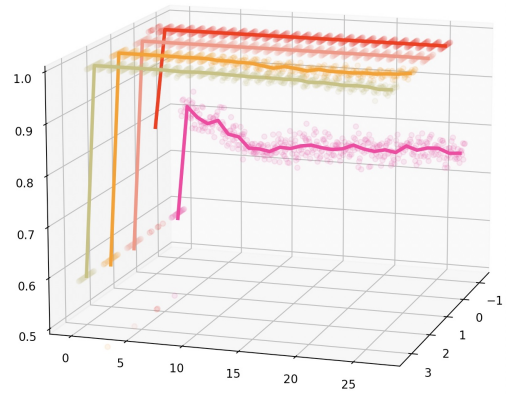


(b) Pearson correlation between attention and logit similarity.

Figure 13: Interpreting attention values from kernel regression perspective on Tweet Eval (Irony) dataset.



(a) Predicting $\arg \max_o P(o|x_i)$ with *key* vectors.



(b) Predicting y_i with *value* vectors.

Figure 14: Investigating information in key and value vectors on Tweet Eval (Irony) dataset.

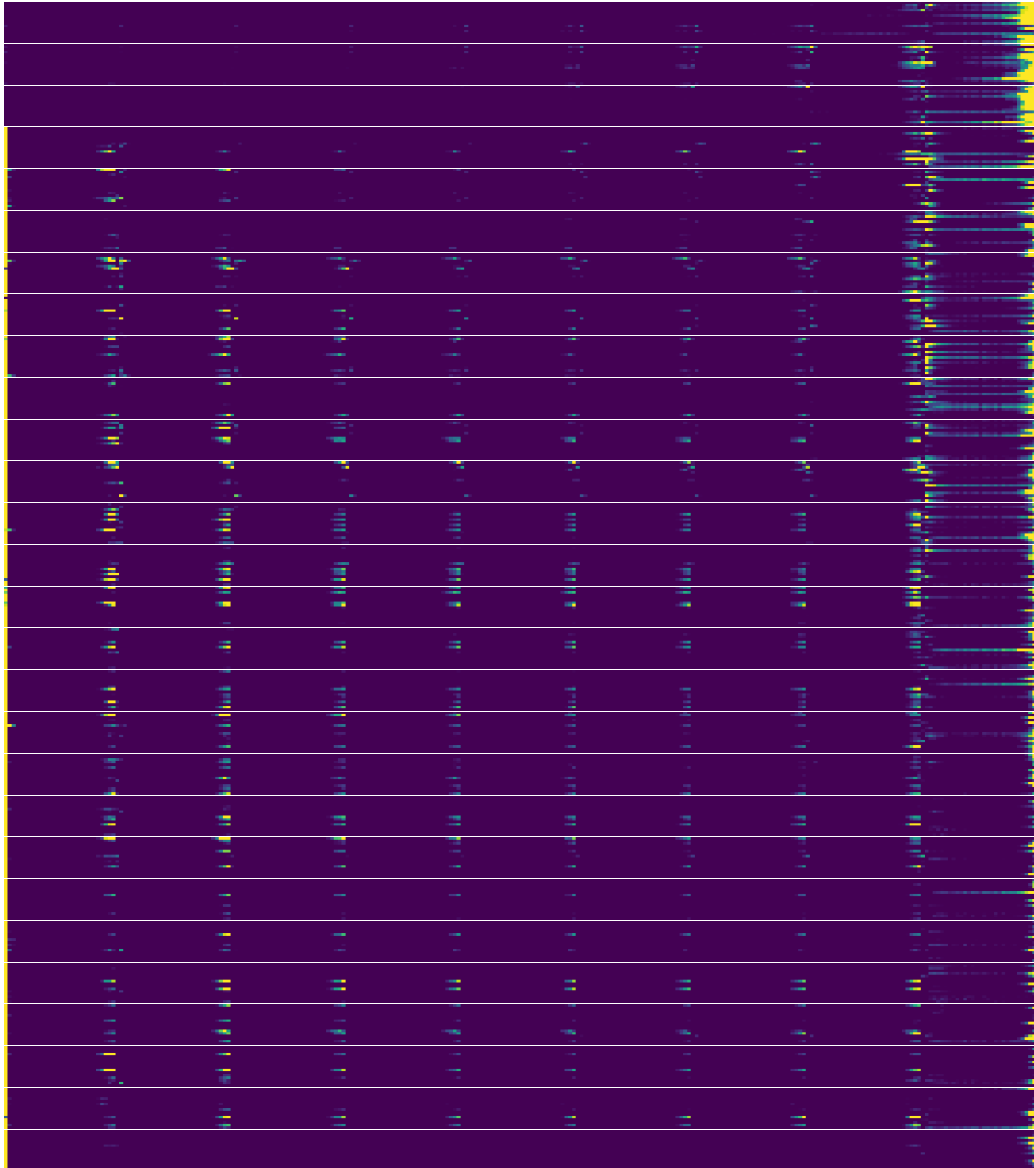
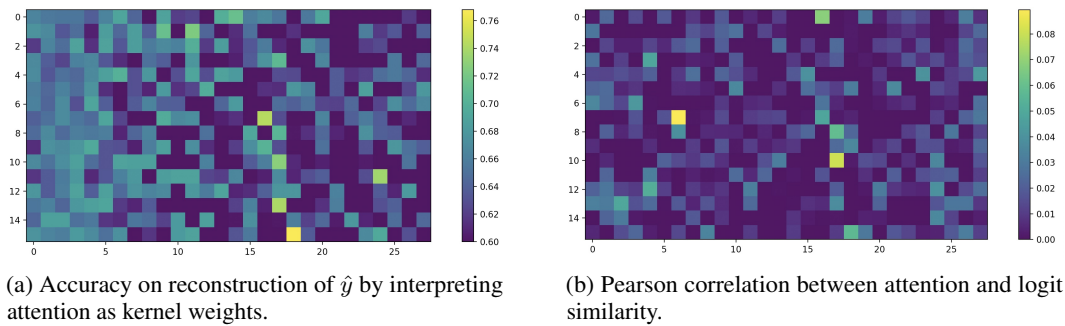


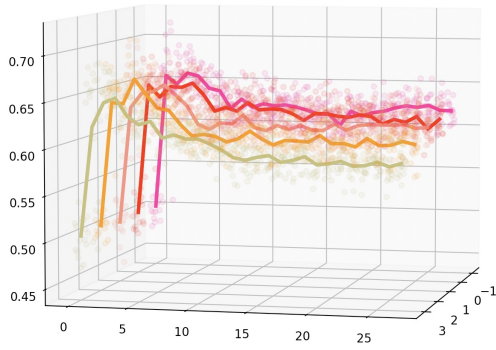
Figure 15: Averaged attention map over Tweet Eval (Offensive) test set.



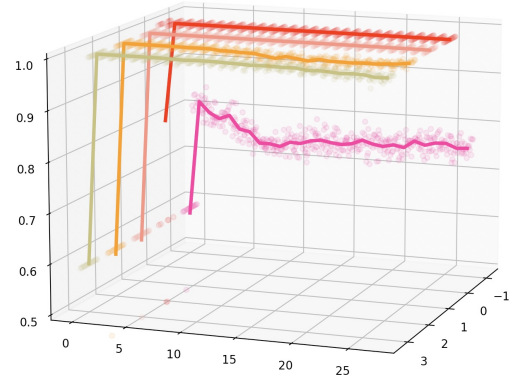
(a) Accuracy on reconstruction of \hat{y} by interpreting attention as kernel weights.

(b) Pearson correlation between attention and logit similarity.

Figure 16: Interpreting attention values from kernel regression perspective on Tweet Eval (Offensive) dataset.



(a) Predicting $\arg \max_o P(o|\mathbf{x}_i)$ with *key* vectors.



(b) Predicting y_i with *value* vectors.

Figure 17: Investigating information in key and value vectors on Tweet Eval (Offensive) dataset.

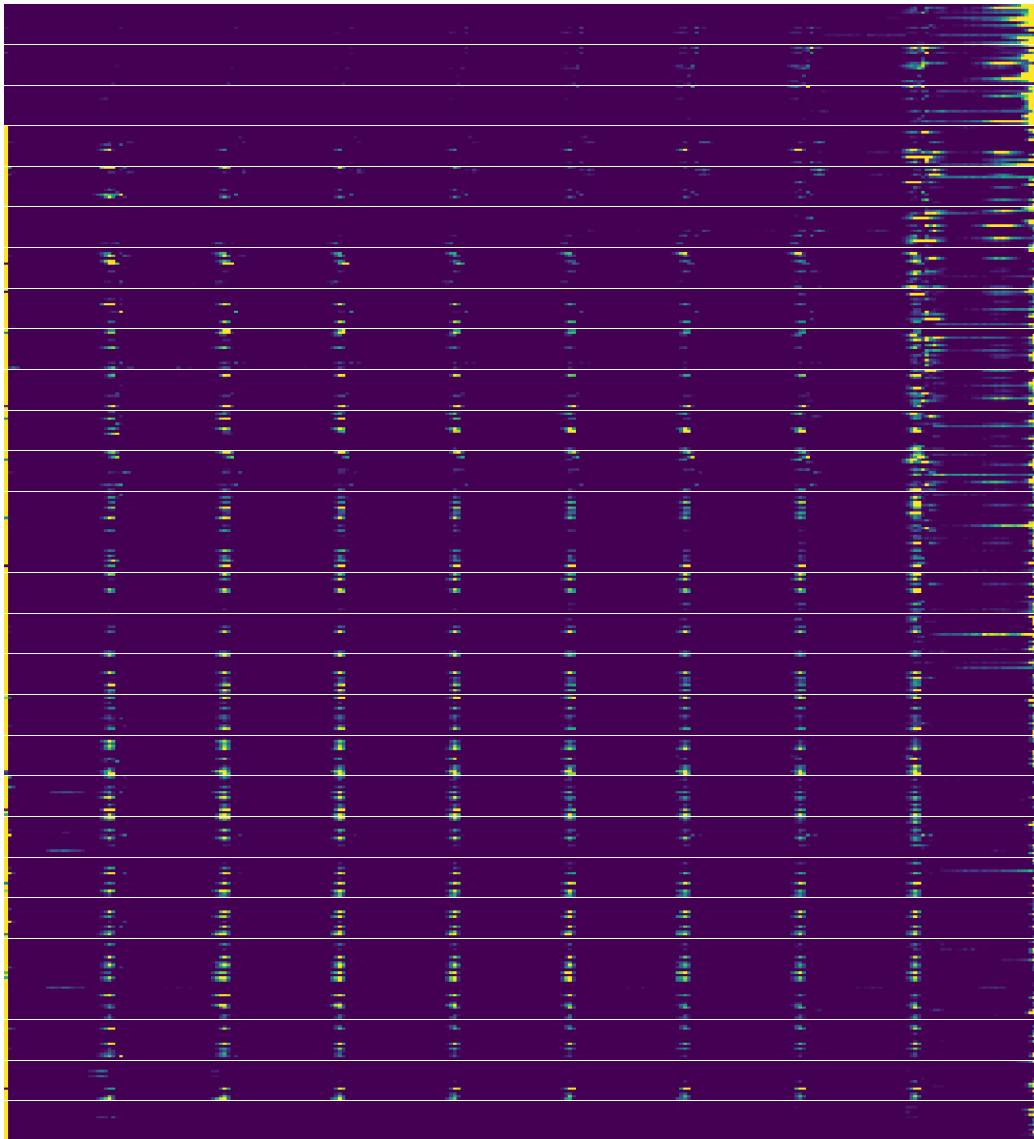
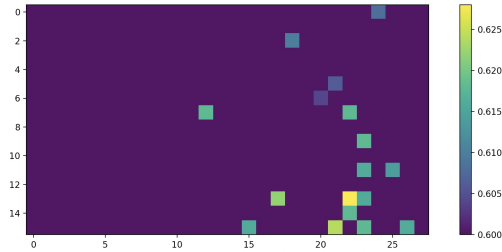
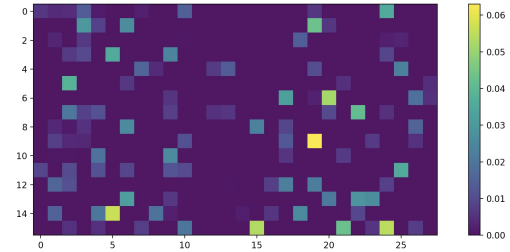


Figure 18: Averaged attention map over MNLI test set.

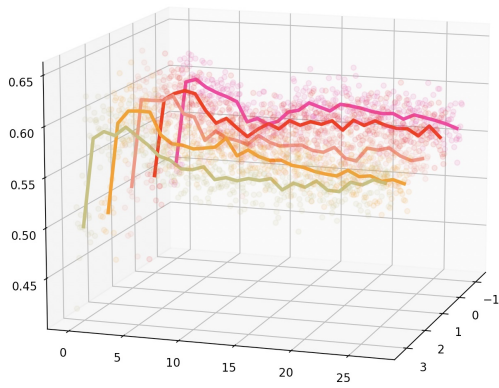


(a) Accuracy on reconstruction of \hat{y} by interpreting attention as kernel weights.

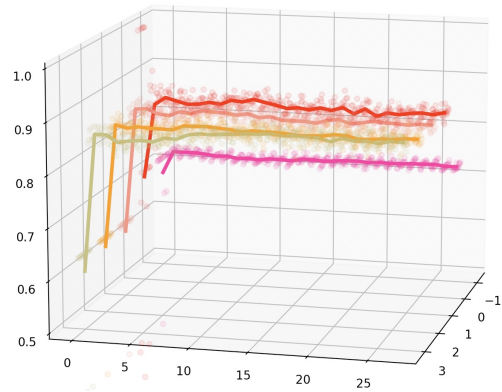


(b) Pearson correlation between attention and logit similarity.

Figure 19: Interpreting attention values from kernel regression perspective on MNLI dataset.



(a) Predicting $\arg \max_o P(o|\mathbf{x}_i)$ with *key* vectors.



(b) Predicting y_i with *value* vectors.

Figure 20: Investigating information in key and value vectors on MNLI dataset.